Reactions of Complex Ligands, Part 89[+]

Incorporation of Chromium Carbenes in a Silica Matrix by Sol–Gel Processing: Application to Aminolysis of Alkoxycarbene Complexes

Simone Klapdohr,*[a] Karl Heinz Dötz,*[a] Wilfried Assenmacher,[b] Wilfried Hoffbauer,[b] Nicola Hüsing,[c] Martin Nieger,[b] Jürgen Pfeiffer,[c] Michael Popall,[d] Ulrich Schubert,[c] and Gregor Trimmel[c]

Dedicated to Professor Günter Wulff on the occasion of his 65th birthday

Abstract: Chromium carbene complexes have been immobilized in a silica matrix by sol–gel processing based on the polycondensation of (trialkoxy)silylethylphosphane ligands and tetraalkoxysilanes. The microstructure of the material obtained depends on the gelation conditions. In situ gelation of alkoxy- or aminocarbene complexes with tetramethoxysilane (TMOS) affords mesoporous materials with a homogeneous distribution of the metal complex. The metal carbene moiety is accessible for small substrates as demonstrated for the aminolysis of the incorporated methoxy(phenyl)carbene complex which slows down with increasing bulk of the amine.

Keywords: aminolysis reactions · carbene complexes · chromium · immobilization · sol–gel processes

Introduction

Over the past 20 years Fischer-type metal carbenes $(CO)_5M{=}C(R^1)XR$ (e.g. M = Cr; X = O, NR)[2] have found a multi-facetted application in organic synthesis.[3] Based on the isolobal analogy[4] of the pentacarbonyl metal fragment and an oxygen atom their reactivity parallels that of organic carbonyl compounds such as carboxylic esters or amides. Reflecting the pronounced acceptor properties of the metal carbonyl fragment, alkyl(alkoxy- or amino)carbene complexes reveal an enhanced α-CH acidity[5] which has been exploited in stereoselective carbon–carbon bond formation such as in aldol[6] and Michael addition reactions.[7] Moreover, alkenylcarbene ligands are excellent dienophiles and dipolarophiles for [4+2] and [3+2]cycloaddition reactions.[3b, 8] Beyond these ligand-centered reactions the metal carbonyl moiety provides an efficient template for both stoichiometric and catalytic metal-centered cycloaddition reactions as demonstrated for chromium-mediated diastereoselective stoichiometric benzannulation[9] and catalytic cyclopropanation reactions[10]. Further encouraged by the impact of metal–carbene catalyzed olefin metathesis on the synthesis of functionalized middle-sized rings and macrocycles[11] we became interested in the immobilization of carbene complexes, and we focused on the incorporation of the metal carbene functionality into a porous silica gel network.

Immobilization of organometallic compounds as increasingly applied for homogeneous catalysts has become a field of growing interest during the last two decades.[12] This strategy combines the advantages of homogeneous catalysts characterized by their molecular nature with the enhanced thermostability and easy separation of heterogeneous catalysts. Chromium carbene complexes are of special interest as retainable catalysts and as starting materials for solid state synthesis. Recently, Fischer carbene complexes have been attached to cross-linked polystyrene.[13] However, inorganic supports are superior to organic supports with respect to thermal and mechanical stability.[12b] Due to the higher rigidity

[a] S. Klapdohr, Prof. Dr. K. H. Dötz
Kekulé-Institut für Organische Chemie und Biochemie
der Universität Bonn
Gerhard-Domagk-Strasse 1, 53121 Bonn (Germany)
Fax: (+49)228-73-5813
E-mail: doetz@uni-bonn.de

[b] Dr. W. Assenmacher, Dr. W. Hoffbauer, Dr. M. Nieger
Institut für Anorganische Chemie der Universität Bonn (Germany)

[c] Dr. N. Hüsing, Dr. J. Pfeiffer, Prof. Dr. U. Schubert, G. Trimmel
Institut für Anorganische Chemie der Technischen Universität Wien
Getreidemarkt 9, 1060 Wien (Austria)

[d] Dr. M. Popall
Fraunhofer Institut für Silicatforschung
Neunerplatz 2, 97082 Würzburg (Germany)

[+] Part 88, see ref. [1].

Supporting information for this article, available on the WWW under http://www.wiley-vch.de/home/chemistry or from the author.

  0947-6539/00/0616-3006 $ 17.50+.50/0

of the inorganic polymer matrix the reaction conditions (solvent, temperature) can be varied over a broad range which allows a better control of the structure or microstructure of the matrix. The rigid framework minimizes the interactions of the immobilized complexes with neighboring functional groups which might result in deactivation processes.

The sol–gel method[14] is an attractive choice for the heterogenization of metal complexes.[15] The in situ incorporation of the complex into the polymer matrix allows a higher loading than achieved by other methods,[16] since the bonding of the metal centers is not restricted to the exterior surface of the macroporous particles, and the active sites are homogeneously distributed throughout the body of the inorganic polymer. Since the structure of the matrix, as defined by porosity, surface area, and flexibility, can be controlled by the reaction conditions, the active sites of the inner surface may remain accessible for the substrates. We now report on the immobilization of chromium carbenes incorporated into a silica gel matrix through covalent bonds and on our efforts to control the microstructure of these materials in order to exploit them in reactions occurring at the metal carbene fragment.

Synthetic strategy: Metal complexes may be anchored to a silica-gel matrix by polycondensation of tetraalkoxysilanes with appropriate alkoxysilanes $(RO)_3Si{-}X{-}D$, where X is a chemically inert spacer such as a $(CH_2)_n$ chain and D represents a functional group suited for complexation of a metal[12] (Scheme 1). The properties of the gels doped with metal complexes depend on the nature and the concentration

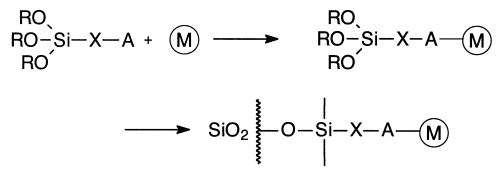

M = coordinatively unsaturated metal complexes

D = functional group suitable for coordination to metal centers

X = chemically inert spacer $(CH_2)_n$

Scheme 1. Strategy for the immobilization of metal complexes by sol–gel processing.

Abstract in German: *Chrom-Carben-Komplexe wurden in einer Silicagel-Matrix durch Polykondensation von (Trialkoxy)silylethylphosphan-Liganden und Tetraalkoxysilanen über den Sol-Gel-Prozeß immobilisiert. Die Mikrostruktur der erhaltenen Materialien hängt von den Vergelungsbedingungen ab. Die in situ-Vergelung der Alkoxy- oder Aminocarbenkomplexe mit Tetramethoxysilan (TMOS) liefert mesoporöse Materialien, die eine homogene Verteilung des Metallkomplexes aufweisen. Die Metall-Carben-Funktion ist für kleine Substrate erreichbar, wie die Aminolyse des Methoxy(phenyl)carbenkomplex-Gels zeigt, die mit steigendem Raumanspruch des Amins verlangsamt wird.*

of the precursors as well as on the reaction conditions such as pH and temperature which are known to influence the hydrolysis and the condensation reactions of alkoxysilanes leading to structural variations of the polycondensation products.[14b,c, 17]

Our interest in synthetic applications of Fischer metal carbenes led us to explore whether this type of organometallic compound is compatible with the experimental conditions applied in the sol–gel process.

Results and Discussion

Immobilization of the carbene complex: The strategy for the immobilization of the chromium carbene is based on the coordination of a phosphine ligand bearing an alkyltri(alkoxysilyl) substituent which is suited for the polycondensation with a tetraalkoxysilane.

The synthesis of the (trialkoxysilyl)ethyldiphenylphosphine chromium carbene complexes **4** and **5** proceeded in two steps: First, the phosphine ligand bearing trimethoxy- (**2**) or triethoxysilyl (**3**) substituents was prepared following a modified protocol based on the addition of diphenylphosphine to equimolar amounts of (trialkoxy)vinylsilane in the presence of azobis(isobutyronitrile) at 110 °C.[18] In a second step, the phosphine ligand **2** or **3** was coordinated to the chromium methoxy(phenyl)carbene complex **1** by photodecarbonylation at −30 °C[19] (Scheme 2) affording *cis/trans* (3:1) mixtures of phosphine carbene complexes **4** and **5**, respectively. The ethoxysilyl complex **5** was isolated as a red solid, while the methoxysilyl analogue **4** was obtained as a viscous oil.

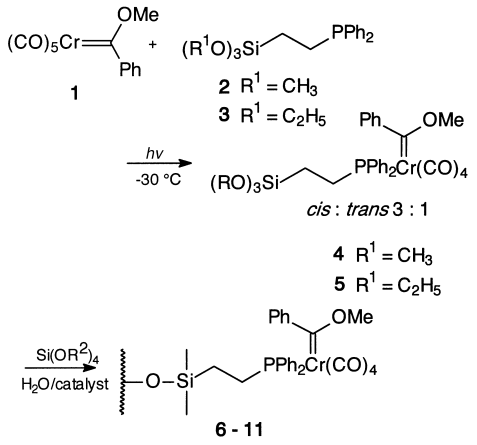

	Catalyst	Precursor complex	R^2
6	NH_4OH	**5**	C_2H_5
7	NaF	**5**	C_2H_5
8	NH_4OH	**5**	CH_3
9	NaF	**5**	CH_3
10	NH_4OH	**4**	CH_3
11	NaF	**4**	CH_3

Scheme 2. Immobilization of **1** on silica by sol–gel processing.

  0947-6539/00/0616-3007 $ 17.50+.50/0

The polycondensation of phosphine metal carbenes **4** and **5** with excess (15 equiv) tetraalkoxysilane was carried out in the presence of an aqueous catalyst which provided the equimolar amount of water required for the hydrolysis of all alkoxysilyl groups. The choice of the catalyst is crucial in two aspects; first, it governs the microstructure of the inorganic network, and second it must be compatible with the metal carbene complex. Three different types of catalysts were tested: Acetic acid (0.1 wt% in H_2O) led to decomposition of the carbene complex[20] as indicated by the disappearence of the characteristic ν(CO) absorptions in the IR spectrum of the tetracarbonyl carbene complex as well as by the disappearence of the typical red color of the complex even before gelation occurred. In contrast, both ammonium hydroxide (0.1 wt% in H_2O) and sodium fluoride (0.1 wt% in H_2O) turned out to be suitable catalysts; gelation occurred within 1.5 h or 15 min, respectively. The gels obtained were aged at room temperature for five days in order to stabilize the gel network before the solvent was removed in vacuo.

For purification purposes and in order to study the leaching behavior, the resulting gels were washed several times with diethyl ether in which the precursor complexes **4** and **5** show excellent solubility. Almost no leaching was detected from gel **11** when tetramethoxysilane (TMOS) and the (trimethoxysilyl)ethyldiphenylphosphine carbene complex **4** were used as starting materials under NaF catalysis. Other combinations of tetraalkoxysilane and phosphine carbene complexes **4** and **5** as well as the use of ammonium hydroxide as catalyst resulted in significant leaching as indicated by the color and the IR spectroscopic characterization of the washing solution.

The nature of the catalyst may dramatically influence the gelation process, and therefore the application of different catalysts is expected to lead to significant variations in the properties of the resulting gels.[17a] At low pH values linear chain growth is preferred, while a microstructure with large spherical particles is observed for the base-catalyzed gel formation resulting in lower shrinkage and higher porosity. Gelation times and properties do not only depend on the pH of the solution, but also on the mechanism of the catalytic process. We focussed on the catalysis by hydroxide and fluoride ions which occurs by a mechanism involving nucleophilic attack at the silicon center as the initial step; this results in spherical particles. However, the microstructure of the final xerogels changes under different pH conditions (acidic or basic), which results in different reaction kinetics both for hydrolysis and condensation. For the fluoride-catalyzed system hydrolysis and condensation are much faster leading to a network with smaller spherical particles. As a consequence of the accelerated sol–gel reactions by fluoride catalysis a more completely condensed network is obtained after five days of aging; most of the functionalized trialkoxysilanes are incorporated by chemical bonding, resulting in a lower degree of leaching during the following washing processes.

The analytical characterization of the dried gels **8**–**11** as determined by X-ray fluorescence reveals that the molar Cr:P:Si ratios significantly vary with the trialkoxysilyl substitution pattern in the phosphine carbene complex precursors and the catalyst used for the condensation (Table 1). Only the data for the materials **10** and **11** derived from TMOS and the (trimethoxy)silylethylphosphine complex precursor **4** are in satisfactory agreement with the Si:P and Si:Cr ratios calculated for a complete condensation of the complex precursor on the silica matrix. Ammonium hydroxide and sodium fluoride both turned out to be efficient catalysts. These results indicate that the carbene complex can be incorporated nearly quantitatively into the gel network under these conditions. They are consistent with previous observations[21] that TMOS is a more reactive component in the sol–gel process than its ethoxy analogue TEOS.

Table 1. X-ray fluorescence analysis of the gels obtained from precursor complexes **4** and **5** under hydroxide and fluoride catalysis.

Gel	Molar ratios		
	Si:Cr	Si:P	Cr:P
8	45:1	36:1	0.8:1
9	68:1	69:1	1.0:1
10	11:1	21:1	2.0:1
11	15:1	25:1	1.7:1
	16:1[a]	16:1[a]	1.0:1[a]

[a] Theoretical values, calculated on the basis of complete condensation of both $R'Si(OR)_3$ and $Si(OR)_4$.

The molar Cr:P ratios, which indicate the stability of the carbene and phosphine to chromium bonds under the reaction conditions of the sol–gel process, vary between 1 and 2, and suggest that the cleavage of the phosphine ligand may become an important undesired side reaction as demonstrated for the trimethoxysilylphosphine complex. A comparison of the different catalysts for the polycondensation reactions, ammonium hydroxide and aqueous sodium fluoride, revealed the latter one afforded better molar Cr:P ratios. The high relative chromium content may reflect decomposition of the complex and immobilization of the chromium assisted by the hydroxy groups of the network followed by leaching of the organic decomposition products by the washing process removing also tetraalkoxysilane oligomers.[22]

A comparison of both trialkoxysilyl precursors reveals that the trimethoxysilyl complex **4** allows a better incorporation of the metal carbene into the gel network than its triethoxysilyl analogue **5**. It has been demonstrated[23] that under base catalysis the self-condensation of TMOS is faster than the cocondensation with alkoxysilyl compounds, resulting in the formation of pure silica gel particles. The trialkoxysilane moiety is hydrolyzed at a later stage of the reaction, and thus is preferentially condensed to the surface of the particles already formed. This cocondensation process should be slower for **5** than for **4** since the hydrolysis of ethoxysilyl groups is slower than for their methoxysilyl congeners. As a consequence, the surface area is decreased and less hydroxy groups might be available, resulting in a lower degree of condensation of the trialkoxysilane. If condensation is not completed an increased aging time is expected to assist additional condensation reactions of the ethoxysilyl ligand to the gel network.

The IR spectra of the gel **11** reveal four ν(CO) absorptions (A_1^1, A_1^2, B_1, B_2) which demonstrates the presence of an

0947-6539/00/0616-3008 $ 17.50+.50/0 *Chem. Eur. J.* **2000**, *6*, No. 16

unchanged tetracarbonyl(carbene)phosphine complex moiety. However, an additional set of less intensive ν(CO) absorption bands characteristic of a pentacarbonyl metal fragment indicates that, to a smaller extent, decomposition of the carbene phosphine complex has occurred during the formation of the gel network. In general, the absorption bands of the incorporated carbonyl complexes are broader than those observed for their molecular precursors **4** and **5**.

A solid-state ^{31}P CP-MAS NMR study of the gel **11** showed the presence of three different phosphorus species. Along with the signal expected for a carbene phosphine complex ($\delta = 52.0$) two other signals are observed indicative for the uncoordinated phosphine ligand ($\delta = -10.0$) and its phosphine oxide oxidation product ($\delta = 38.7$). An additional signal for a pentacarbonylphosphine species could not be detected but might be hidden by the signal at $\delta = 52.0$. Decomplexation and oxidation are common features of phosphine ligands which are immobilized on oxidic supports.[24] The ^{13}C CP-MAS NMR data confirm the presence of both the carbene and the (methoxysilyl)alkylphosphine ligand.

Moreover, a broad, less intense signal is observed in the carbonyl range. Additional information about the structure of the inorganic matrix is provided by ^{29}Si CP-MAS NMR spectroscopy which indicates two separate sets of signals due to the T (trioxysilyl) and Q (tetraoxysilyl) species. The formation of Si-O-Si bonds in a given $Si_{4-n}(OSi)_n$ environment (Q^n) where n denotes the number of Si-O-Si bonds formed results in an upfield shift of about 10 ppm.[25] For **11** CP-MAS ^{29}Si-NMR experiments indicate the formation of a network containing Q^4 ($\delta = -107$) and Q^3 ($\delta = -100$) species along with minor signals of Q^2 ($\delta = -90$) and T^3 species ($\delta = -64$) (Figure 1) resulting from the parent trimethoxysilyl phosphine ligand.

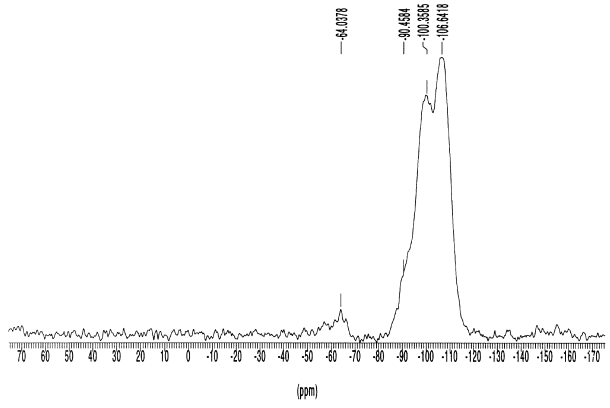

Figure 1. ^{29}Si CP-MAS solid-state NMR spectrum of **11**.

The structure of gel **11** was further characterized by scanning electron microscopy (SEM) and transmission electron microscopy (TEM). Scanning electron micrographs display a relatively smooth surface; neither globular particles nor pores can be observed (Figure 2 top). The samples break in scales, and several layers can be observed; neither clusters nor pores are detectable in the TEM micrographs (Figure 3 top).

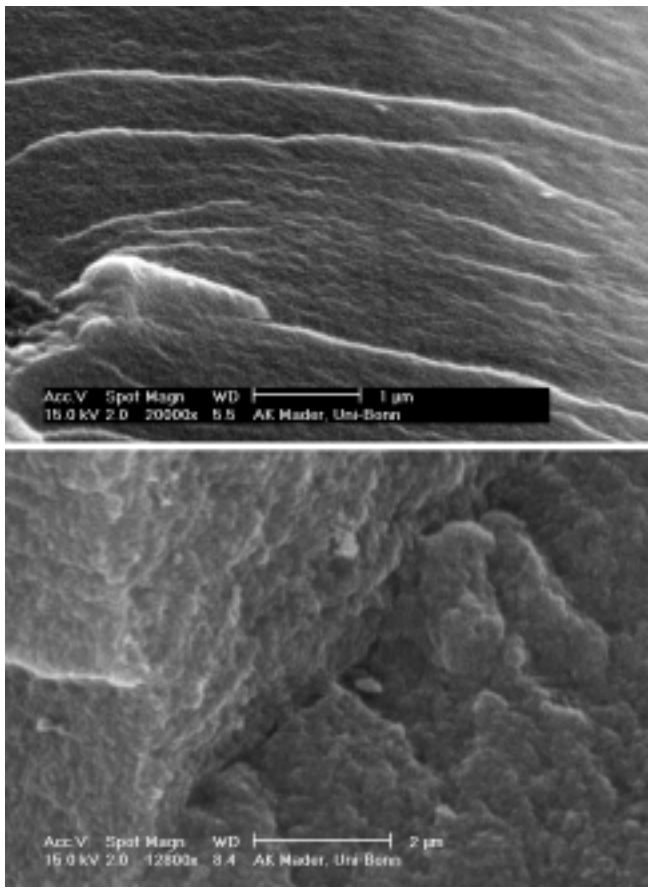

Figure 2. Top: Scanning electron micrograph of **11**. Bottom: Scanning electron micrograph of **12**.

X-ray diffraction (XRD) studies from selected areas of the sample indicate the completely amorphous character of the material; no hints for a long-range order are detected in either the high-resolution lattice images or the electron diffraction patterns. The gel **11** appears macroscopically homogeneous. Energy-dispersive X-ray analysis (EDX) on about a 200 nm scale substantiates the presence of the elements of silicon, oxygen, chromium, phosphorus, and carbon. Different areas from the particles reveal constant metal and phosphorus concentrations. The metal compounds are distributed regularly indicating that no separation of the two starting compounds has occurred during the condensation process; a similar conclusion can be drawn from an electron energy loss spectroscopy (EELS) study with a spot analysis using a 10 nm beam. In all EEL spectra, the $Cr-L_{2,3}$ and the $P-L_{2,3}$ edges appear with nearly identical ratios. A quantification of the elements was hampered due to the intense oxygen K ionization edge characterized by a very similar energy loss as observed for the $Cr-L_{2,3}$ edge. The formation of aggregates consisting of metal-containing moieties on a molecular level cannot be excluded.

Optimization of gelation conditions: In order to minimize decomposition of the immobilized carbene complexes we optimized the conditions for the formation and the aging process of the gels. When gelation and aging were carried out

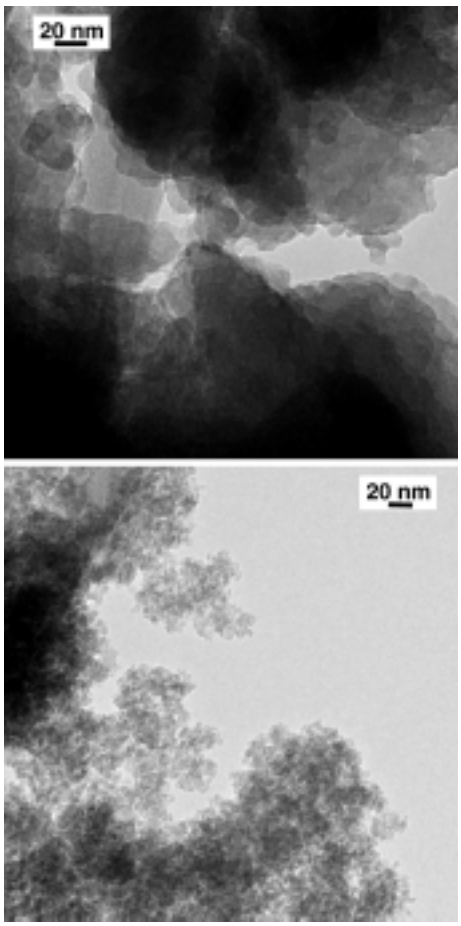

Figure 3. Top: Transmissiom electron micrograph **11**. Bottom: Transmission electron micrograph of **12**.

at lower temperature (2 °C) decomposition decreased; on the other hand, hydrolysis and condensation were also slowed down leading to an incomplete formation of the gel network which resulted in an increased leaching of the complex even though the aging period was extended to 10 days.

The rate of the polycondensation is solvent-dependent.[26] Increased amounts of ethanol as solvent slow down the overall process of both hydrolysis and condensation. With the aim of accelerating the condensation reaction, we changed the solvent while keeping all other parameters constant. If ethanol was replaced by methanol transesterification of the methoxysilyl groups to their ethoxysilyl homologues, which show lower reaction rates, should be avoided; however, decomposition of the complex increased again.

Another aim was to control and increase the pore sizes of the gel which are dependent on the aging conditions.[27] During the aging time a reverse esterification reaction may occur in addition to hydrolysis and polycondensation. Since convex surfaces are more soluble than concave surfaces,[28] an overall mass transport is expected to occur from convex to concave areas. This process favors a neck formation between particles, and is suited to fill up smaller pores thus increasing both the homogeneity of the gel network and the matrix strength. Aging for longer periods of time increases the size and uniformity of the pores.[27] Aging for three days reduced the decomposition of the carbene complex, as indicated by less intense pentacarbonyl bands in the IR spectra of the gel, but also increased the leaching of the complex as well as the shrinkage of the solid after drying due to a less condensed network. After aging for seven and ten days, the decomposition increased significantly. Therefore aging for five days seems to be the conditions of choice in order to simultaneously minimize both the leaching and decomposition process of the carbene complex.

The specific surface area could also be increased by raising the molar ratio of TMOS to the carbene (silylphosphine) complex.[17c] Thus, gels with different molar TMOS/complex ratios were prepared ranging from 15:1 to 50:1, and compared with a gel obtained under the same conditions from pure TMOS in the absence of carbene complex **4**. X-ray fluorescence analysis reflects the TMOS/complex ratios in the resulting gel as indicated by the Si:Cr and Si:P ratios (Table 2). We used our standard conditions (room temperature, same kind and amount of catalyst, ethanol as solvent, aging for five days) for all experiments in order to eliminate side effects arising from parameters other than the TMOS/complex molar ratios. The products still contained undetermined amounts of water and/or uncondensed hydroxy groups.

Increasing the TMOS/complex molar ratio allows one to reduce the shrinkage that occurs upon drying of the wet gel presuming the formation of a more stable network. Unfortunately, decomposition of the complex is also favored by an increasing molar ratio of TMOS/**4**; for instance, a 50:1 ratio induces almost complete decomposition, as demonstrated by the decrease of the characteristic tetracarbonyl absorption bands in the IR spectra along with the increase in bands indicative of hexacarbonylchromium and pentacarbonylchromium complexes. This leads to the conclusion that the decomposition gradually increases with the concentration of the hydroxy groups present in the silica matrix.

Table 2. X-ray fluorescence analysis of the gels obtained from precursor complex **4** under fluoride catalysis.

Molar ratio TMOS/**4**	ratio Si:Cr	ratio Si:P	ratio Cr:P
30:1	18:1	35:1	2.0:1
20:1	10:1	23:1	2.2:1
15:1	9.5:1	18:1	1.9:1
15:1[a]		19.5:1	

[a] Molar ratio TMOS/**2**.

A study of the specific surface area by nitrogen sorption measurements according to the Brunauer–Emmett–Teller (BET) method (Table 3) revealed that the surface increases with the molar ratio of TMOS/**4**. While the aging period when extended from three to ten days had only a marginal effect, a significant increase of the specific surface occurred upon raising the TMOS/**4** ratio from 15:1 to 30:1.

According to the original Brunauer–Deming–Deming–Teller (BDDT) classification[29] the nitrogen adsorption–desorption isotherms of the gels obtained (Figure 4 top) are characteristic of microporous solids (pore radii $\leq$ 1.5 nm).[14c, 30] This is consistent with the very fine texture as shown by TEM (Figure 2top). The volume adsorbed at the lowest relative

  0947-6539/00/0616-3010 $ 17.50+.50/0 *Chem. Eur. J.* **2000**, *6*, No. 16

Table 3. Specific surface area and pore size by BET measurements of gels obtained with different molar ratios of TMOS/**4**.

Ratio TMOS/complex	Aging	BET surface [$m^2 g^{-1}$] [a]	Average pore volume [$cm^3 g^{-1}$]	Average pore radii [nm]
15:1	3 d	375	0.23	1.2
15:1	10 d	396	0.23	1.16
30:1	5 d	668	0.41	1.2
100:0	5 d	908	0.69	1.5

[a] The inaccuracy of the measurements is assumed to be 10%.

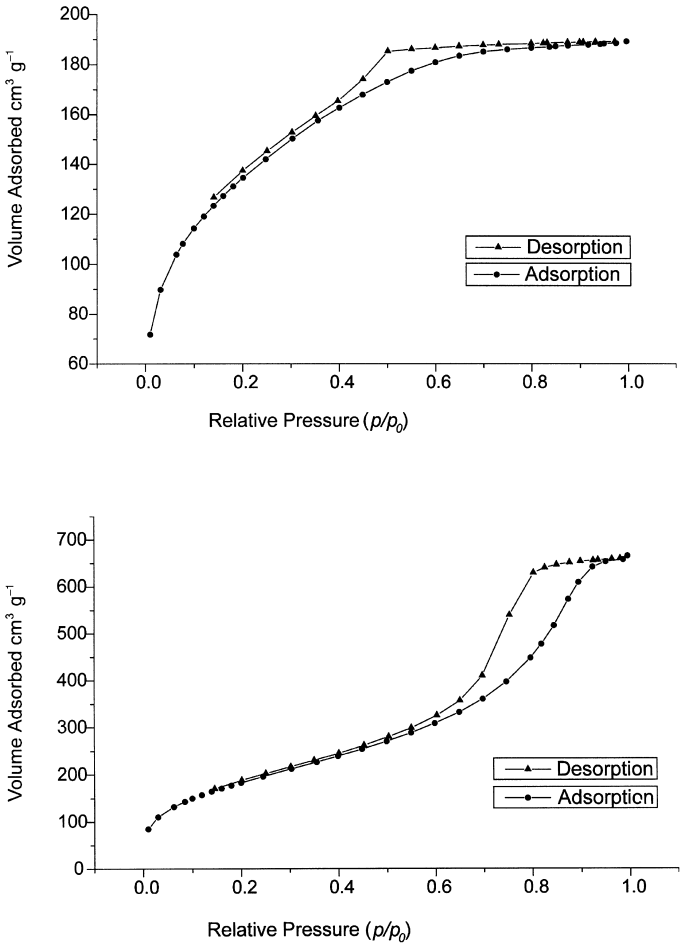

Figure 4. Top: Nitrogen sorption isotherms of **11**. Bottom: Nitrogen sorption isotherms of **12**.

pressure represents about 37% of the total pore volume indicating a large amount of extremely small pores. Nitrogen sorption measurements provided additional information on the specific pore volume and the distribution of the pore radii. The pore volumes and pore radii listed in Table 3 are averaged values and do not imply the predominance of such pores. The pore size distributions calculated by differentiation of the pore volume adsorbed or desorbed with respect to the pore size by the method of Barrett, Joyner, and Halenda (BJH method)[31] do not reveal any maximum; this result suggests a broad distribution of pore sizes.

Aging in silane solution: The network of wet gels can be strengthened and stiffened by providing additional monomers to the alcogel after gelation by aging in a TEOS solution. The resulting xerogels revealed properties similar to those of aerogels obtained by supercritical drying conditions which provide highly porous materials with extremely low density.[17e,f] We modified these conditions and added a solution of 70% TEOS in ethanol to the gel, prepared from TMOS and complex **4** under fluoride catalysis, 20 min after gelation had occurred. The resulting gel **12** underwent a significantly less pronounced shrinkage as observed after evaporation of the solvent and drying. But again owing to a higher Si–OH concentration decomposition increased.

Despite that some structural features changed significantly. The nitrogen adsorption–desorption isotherms of this gel are typical for mesoporous materials (pore radii 1.5–50 nm) (Figure 4 bottom).[14c, 30] The BET surface area is increased to 592 $m^2 g^{-1}$; the pore size distribution shows a new maximum at a pore diameter of 7–8 nm in the BJH desorption curve. Apart from this narrow pore size distribution in the mesoporous range, a limited number of micropores exist reducing the average BET pore diameter to 6.2 nm. The modified structure of the gel is further confirmed by SEM and TEM images (Figures 2 bottom and 3 bottom). As demonstrated by SEM, the surface and edges of fracture pieces of the sample seem to be composed of very small particles leading to a rough, scale-like structure of the surface and the fracture. TEM reveals agglomerations of small randomly packed particles of approximately 15 nm in diameter. Particles up to 50 nm are resolved by electron microscopy.

Aminolysis reactions: We were interested in whether the immobilized metal carbenes are still accessible and reactive towards nucleophiles within the pores of the network. To test their reactivity we focussed on the aminolysis reaction of methoxycarbene complexes[32] which in solution generally occurs rapidly under mild conditions. For an evaluation of the reaction in the solid phase we first studied the aminolysis with the ethoxysilylphosphine precursor **5** in solution. This complex, a solid which is easy to handle and to purify, provides—apart from the metal-coordinated carbene carbon atom—with the silicon an additional potential target for nucleophilic attack. However, we found that the addition of the amine exclusively occurred at the carbene carbon atom under our standard conditions. We chose ammonia, which represents the least bulky amine, as a qualitative reference nucleophile. It added readily to methoxycarbene complex **5** at $-65\,^{\circ}C$ within one hour to give a 57% yield of aminocarbene complex **13** (Scheme 3). We then compared the reactivity of ammonia with that of more bulky primary amines such as allylamine and isobutylamine, and further included pyrrolidine as a representative secondary amine. A qualitative study demonstrated that the rate for the aminolysis reaction is mainly governed by steric requirements in the tetrahedral intermediate formed upon addition of the nucleophile to the carbene carbon atom; the relative rate decreased in the order of ammonia, primary amines, and pyrrolidine.[34] This order of reactivity was confirmed by independent competition experiments carried out at low temperature in homogeneous ethereal solution with the precursor complex **5** and excess equimolar amounts (10 equiv) of allylamine, isobutylamine,

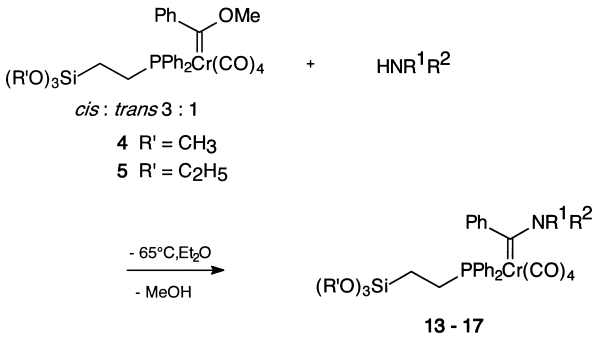

	HNR^1R^2	R′
13	ammonia	Et
14	allylamine	Et
15	allylamine	Me
16	isobutylamine	Et
17	pyrrolidine	Et

Scheme 3. Aminolysis reactions of the precursor complexes **4** and **5**.

and pyrrolidine. ^{1}H NMR analysis demonstrated that aminocarbene complexes **14**, **16**, and **17** were formed in a 3.3:3.3:1 ratio when the reaction was performed at $-60\,^{\circ}$C; a 2.5:2:1 ratio was observed at $-30\,^{\circ}$C. Based on these results allylamine may be regarded as slightly more reactive than the more bulky isobutylamine, while the secondary amine pyrrolidine is distinctly less reactive. The molecular structures of the amino- and allylaminocarbene complexes **13** and **14** were established by X-ray diffraction (Figure 5a, b) which confirmed the *cis* geometry of carbene and phosphine ligands. The majority of pentacarbonyl carbene complexes adopt solid-state conformations in which the plane of the carbene ligand bisects the angle of the *cis*-$M(CO)_2$ fragment.[35] The molecular structures of aminocarbene complexes **13** and **14** reveal a rather flat potential for the rotation around the metal–carbene bond even in the solid state, and the orientation of the carbene ligand may be controlled by hydrogen bonds formed by N-H donors and either silyloxy or carbonyl oxygen acceptors. The asymmetric unit of allylaminocarbene complex **14** contains two independent molecules that represent two conformers. For conformer a the bisecting angle is reduced to 10° as a result of a weak intermolecular NH bridge (2.6 Å) to a carbonyl ligand between two neighboring identical conformers. The same angle is observed for complex **13** in which hydrogen bonds are formed (2.3 Å) to a carbonyl ligand and a silyloxy group. The absence of hydrogen bonding widens the bisecting angle to 28° as observed for conformer b. The allylamino substituent in complex **14** is disordered but reveals an *E* configuration with respect to the carbene–nitrogen bond (Figure 5b).

Silica gels including a metal aminocarbene are also accessible by an alternative route which is based on the gelation of a tetraalkoxysilane with a suitable aminocarbene complex precursor. We chose the allylaminocarbene complex **15**, an oily compound bearing the (methoxysilyl)phosphine ligand, as a model complex which was subjected to our standard sol–gel conditions using TMOS. This sequence allowed us to evaluate both procedures and compare their

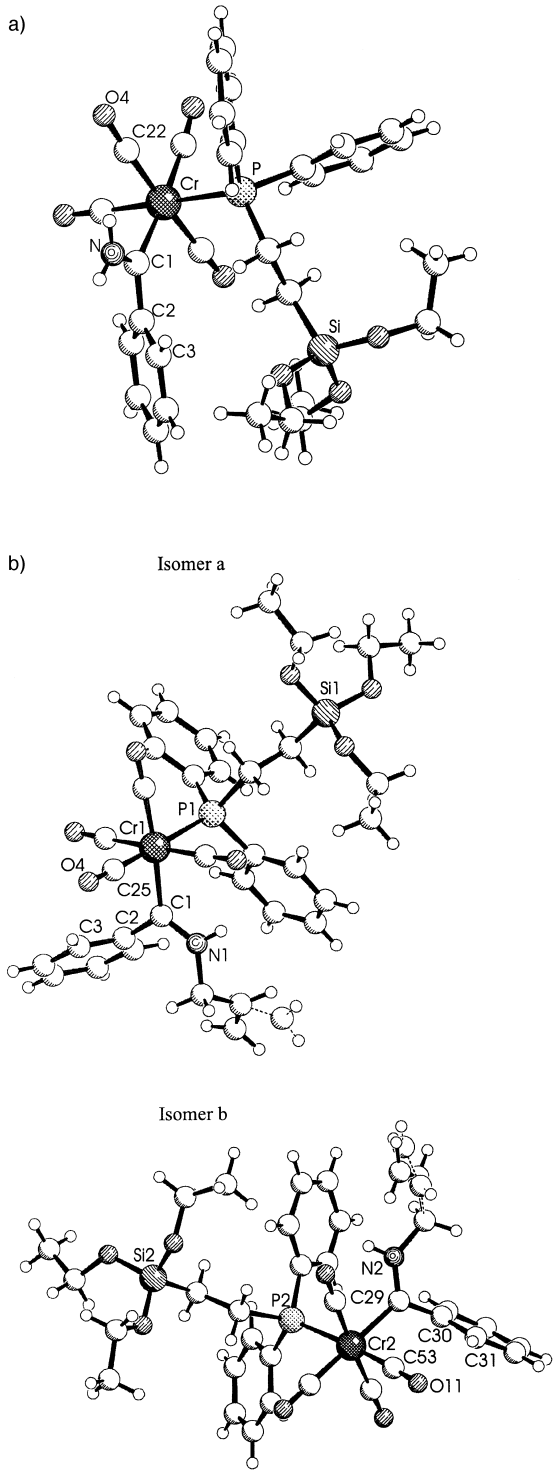

Figure 5. a) Diamond plot of the molecular structure of complex **13**. Selected bond lengths [Å] and angles [°]: Cr–C1 2.0814(14), C1–N 1.3126(19), N–H1A 0.893(14), N–H1B 0.872(14); N-C1-C2-C3 137.03(14), Cr-C1-C2 125.35(10), C1-Cr-P 89.80(4), C22-Cr1-C1-C2 80.47(12). b) Diamond plot of the molecular structure of complex **14**. The crystal contains two isomers which again consist of two conformers with different conformations of the allyl group. The difference in the structure is shown by black and dashed bonds in the allyl group. Selected bond lengths [Å] and angles [°]: isomer **a**: Cr1–C1 2.091(2), C1–N1 1.315(3), N1–H1 0.883(17); N1-C1-C2-C3 112.5(2), Cr-C1-C2 121.46(14), C1-Cr1-P1 96.43(6), C25-Cr1-C1-C2 76.21(17); isomer **b**: Cr2–C29 2.092(2), C29–N2 1.309(3), N2–H2 0.874(17); N2-C29-C30-C31 – 69.2(3), Cr2-C29-C30 122.53(15), C29-Cr2-P2 94.51(6), C53-Cr2-C29-C30 61.39(17).

0947-6539/00/0616-3012 $ 17.50+.50/0 *Chem. Eur. J.* **2000**, *6*, No. 16

efficiencies by monitoring the color changes and IR spectra during the condensation and aging processes.

The gel **18** prepared from the aminocarbene precursor **15** and TMOS (Scheme 4) had the same yellow color as the precursor complex in solution. The IR spectrum of the gel

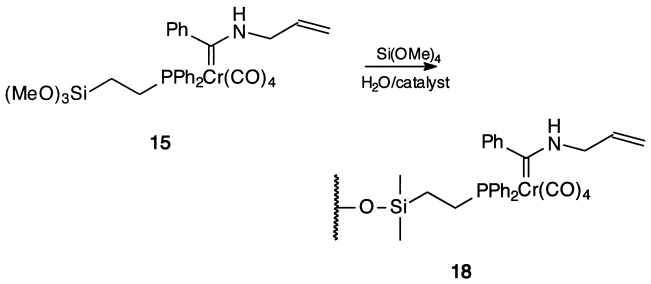

Scheme 4. Immobilization of **15** on silica by sol–gel processing.

showed, apart from the bands of the tetracarbonyl aminocarbene complex (FT-IR (KBr): $\tilde{\nu} = 2001$ (m, C=O, A_1^2), 1907 (vs, C=O, A_1^1), 1881 cm^{-1} (vs, C=O, B_1, B_2)), the carbonyl bands of a pentacarbonyl aminocarbene complex species (FT-IR (KBr): $\tilde{\nu} = 2057$ (w, C=O, A_1^1), 1941 cm^{-1} (m, C=O, A_1^2, E) which could be washed out to a great extent. The formation of the pentacarbonyl species may be explained in terms of a decarbonylative decomposition of the tetracarbonyl carbene (ethoxysilyl)phosphine complex upon reaction with the hydroxy groups of the surface[33] providing excess CO required for the substitution of the phosphine ligand to afford the pentacarbonyl species.

Aminolysis of the methoxyphenylcarbene complex in the gel **11** led to the corresponding aminocarbene complexes (Scheme 5). As known from the behavior in solution, the IR tetracarbonyl absorption pattern exhibits a bathochromic shift for the aminocarbene complexes with respect to their methoxy carbene precursors. All aminolysis reactions of gel **11** were accompanied by a color change from red to brown. The brown color might arise from residual methoxycarbene starting material encapsulated in the pores which eluded aminolysis. The fact that the absorption pattern of the pentacarbonyl impurity present in the gel remained unchanged upon the aminolysis indicates that the pentacarbonyl species represents the pentacarbonyl phosphine complex rather than the pentacarbonyl carbene complex.

The aminolysis reactions in the gel are slower than the corresponding reactions in solution. This is not surprising since the amine has to diffuse into the narrow pores to access the carbene complex. Whereas in solution aminolysis with primary amines occurs readily at $-78\,^{\circ}C$ the gel suspended in diethyl ether has to be warmed up slowly to $-25\,^{\circ}C$. Despite of the increased temperature the reactions of the gels required several hours (ammonia) to several days (primary and secondary amines). Reaction with the secondary amine pyrrolidine was not completed even after three days; the shoulder of the A_1^2 band ($\tilde{\nu} = 2012\ cm^{-1}$) indicative of the methoxycarbene precursor further diminished within another three days. Similarly, isobutylamine reacted more slowly than the less bulky allylamine. These results illustrate that aminolysis reactions occurring in the pores are subject to

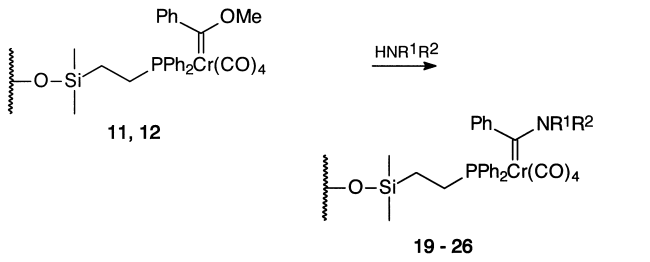

HNR^1R^2	Gel **11**	Gel **12**
ammonia	**19**	**23**
allylamine	**20**	**24**
isobutylamine	**21**	**25**
pyrrolidine	**22**	**26**

Scheme 5. Aminolysis of the carbene complex in the xerogel.

significant diffusion effects, and their rate increases with decreasing bulk of the amine.

The additional aging process applied to the gel **12** to give **23**–**26** enhances both the rate and the degree of conversion of the aminolysis reaction. For the reaction of the gel **12** with ammonia a significant color change was observed already after a few minutes; the resulting gel **23** had an orange color, slightly darker than that of the gel prepared from the aminocarbene precursor **15**. In contrast, under identical conditions the gel **11** underwent visible color changes only after 2 h.

Conclusion

Fischer carbene complexes are compatible with the conditions applied for the sol–gel process and, thus, can be immobilized in a silica gel matrix by this methodology. The metal carbene fragments are tethered to the network by complexation of a trialkoxysilyl phosphine ligand providing far stronger bonding than previously achieved by more conventional adsorption of metal carbenes from solution onto a silica surface. The oxidic matrix causes only minor decomposition arising from decarbonylation and ligand substitution processes. The carbene complexes are homogeneously distributed throughout the whole matrix. Based on the rigidity of the gel network and the defined pore volume in the xerogel, the methoxycarbene ligand is accessible for the addition of amine nucleophiles in subsequent aminolysis reactions. Mesoporous materials with a relatively narrow pore size distribution are obtained which undergo an accelerated and more complete reaction with amines when pre-aged in silane solution. This type of metal carbene xerogels may be extended to carbene ligand centered carbon–carbon bond formation resulting from insertion of alkyne nucleophiles into the metal–carbene bond[36] or from $[n+2]$cycloaddition reactions.[3b]

The enhanced decarbonylation of the immobilized complex might be used for cyclization reactions occurring at a low-valent chromium template which are known to be accelerated by adsorption of the reactants onto silica.[37] Finally, the gels offer the possibility of cleaving the reaction products and

removing them while the chromium template is retained in the oxidic polymer. In this case the chromium carbonyl complex can be used as a traceless linker.[38]

Experimental Section

General: All reactions were performed in flame-dried glassware under an atmosphere of argon with standard Schlenk techniques.

^{1}H and ^{13}C NMR spectra in solution were recorded on Bruker AM 250 and DRX 500 spectrometers; ^{31}P NMR spectra were recorded on a Bruker AMX 300 spectrometer. Chemical shifts are given in ppm using tetramethylsilane (for ^{1}H NMR spectra) and phosphoric acid (for ^{31}P NMR spectra) as external references in solution. Solid state ^{13}C and ^{29}Si NMR spectra were recorded on a Bruker DRX 400 at 100.63 MHz and 79.49 MHz, respectively. The samples were spun in a 4 mm rotor at 4 kHz. A cross polarization sequence was used with typical contact times of 1–3 ms (^{13}C) or 10 ms (^{29}Si) and a recycle delay of 3–5 s. Solid-state ^{31}P NMR spectra were recorded at 161.35 MHz on a Varian Unity 400 spectrometer. The (CP) MAS spectra were recorded at spinning frequencies of 4–6.5 kHz, a contact time of 1 ms and a recycle delay of 3 s. FT-IR spectra were obtained on a Nicolet Magna 550 spectrometer. MS(EI) and HR-MS (EI) were recorded on a Kratos MS-50 spectrometer. Elemental analyses were carried out with an Elementaranalysator CHN-O-Rapid (Heraeus). X-ray fluorescence analyses were obtained on a Siemens SRS 3000 wavelength dispersive system. The measurements were carried out on a sliced sample of 6 mm in diameter in helium (inaccuracy 0.2 %). Melting points were recorded with a Büchi SMP 20 and are uncorrected. Nitrogen-sorption measurements were performed with a Micromeritics Sorptomat ASAP 2000 and 2400. Surface areas were calculated according to the BET method at 77.4 K in the partial pressure range of $0.05 < p/p_o < 0.2$. The samples were pretreated (degassed) overnight at 30 °C before each measurement. Pore volumes were calculated according to the BJH theory. SEM was recorded on a Philips XL 20 microscope (W-Filament ($HV_{(max)}$ = 30 kV)) and TEM on a Philips CM 300 FEG UT operating at 297 kV and equipped with a GIF (Getan Imaging Filter) and a slow scan CCD camera. Samples for these measurements were prepared by grinding the dried gels in a mortar and dispersing them on a holey carbon film supported on a copper grid. XRD on powder were recorded with a Philips PW1050 (Bragg-Brentano-Geometry) with $Co_{K\alpha}$ radiation. Precoated sheeds (Merck, $60F_{254}$) were used for TLC; column chromatography was performed with silica gel (Merck, grade 60, 0.062–0.200 mm), dried in vacuo for two days at 200 °C. A high-pressure mercury lamp type TQ 150 Fa. Heraeus was used for photodecarbonylation.

Crystallographic data (excluding structure factors) for the structures reported in this paper have been deposited with the Cambridge Crystallographic Data Centre as supplementary publication no. CCDC-133895 (**13**) and CCDC-133894 (**14**). Copies of the data can be obtained free of charge on application to CCDC, 12 Union Road, Cambridge CB2 1EZ, UK (fax: (+44) 1223-336-033; e-mail: deposit@ccdc.cam.ac.uk).

Starting materials: Diethyl ether and petroleum ether (40/60) were dried by distillation from calcium hydride under argon. Liquid starting compounds were degassed by the freeze pump and thaw technique. Pentacarbonyl-[methoxy(phenyl)carbene]chromium (**1**)[39] and (alkoxysilyl)ethylphosphines **2** and **3**[18] were prepared according to published procedures. All other chemicals were used as received from commercial sources.

***cis/trans*-Tetracabonyl[(2-trimethoxysilyl)ethyldiphenylphosphine][methoxy(phenyl)carbene]chromium(0) (4)**: A solution of carbene complex **1** (1.25 g, 4 mmol) and alkoxysilylphosphine **2** (1.56 g, 4 mmol) in diethyl ether (240 mL) was irradiated with a 150 W mercury lamp for 4.5 h at −30 °C under a flow of argon. The color of the solution changed from orange to dark red. The cold solution was filtered through celite, and the solvent was removed under reduced pressure. Column chromatography under argon at −30 °C (eluent: petroleum ether/diethyl ether = 5:1) afforded *cis* isomer **4** (2.25 g, 3.64 mmol, 85 %) as a dark red viscous oil; R_f = 0.24 (petroleum ether/diethyl ether = 2:1, −28 °C). In solution at room temperature partial isomerization occurred resulting in an equilibrium *cis*/*trans* ratio of 3:1. ^{1}H NMR (500 MHz, C_6D_6): *cis* isomer: δ = 0.75–0.97 (m, 2H; $SiCH_2$), 2.71 (dt, $^2J_{H,P}$ = 12.5 Hz, $^3J_{H,H}$ = 4.5 Hz, 2H; PCH_2), 3.37 (s, 9H; $SiOCH_3$), 3.99 (s, 3H; OCH_3), 6.65–6.70 (m; ArH), 6.92–7.10 (m; ArH), 7.47–7.61 (m; ArH); *trans* isomer: δ = 0.75–0.97 (m, 2H; $SiCH_2$), 2.79 (dt, $^2J_{H,P}$ = 12.3 Hz, $^3J_{H,H}$ = 4.7 Hz, 2H; PCH_2), 3.38 (s, 9H; $SiOCH_3$), 4.06 (s, 3H; OCH_3), 6.65–6.70 (m, ArH), 6.92–7.10 (m, ArH), 7.47–7.61 (m, ArH); ^{13}C NMR (125 MHz, C_6D_6): *cis* isomer: δ = 3.5 (d, $^2J_{C,P}$ = 2.4 Hz, 1C; Si-CH_2), 26.7 (d, $^1J_{C,P}$ = 18.3 Hz, 1C; PCH_2), 50.3 (s, 3C; $Si(OCH_3)_3$), 64.0 (s, 1C; $C(OCH_3)$), 122.4 (s, 1C; $CArC_p$), 128.4–129.0 (m; ArC), 129.3 (d; PArC), 130.3 (d; PArC), 132.6 (d; PArC), 137.7 (d, $^1J_{C,P}$ = 31.2 Hz, 2C; $PArC_{ipso}$), 153.3 (s, 1C; $CArC_{ipso}$), 221.5 (d, $^2J_{C,P}$ = 14.9 Hz, 2C; CO_{cis}), 226.5 (d, $^2J_{C,P}$ = 6.7 Hz, 1C; CO_{trans} to P), 232.5 (d, $^2J_{C,P}$ = 13.9 Hz, 1C; CO_{trans} to C), 348.8 (d, $^2J_{C,P}$ = 13.0 Hz, 1C; $C_{carbene}$); *trans* isomer: δ = 3.4 (d, 1C; Si-CH_2), 26.0 (d, $^1J_{C,P}$ = 19.1 Hz), 50.8 (s, 3C; $Si(OCH_3)_3$), 66.0 (s, 1C; $C(OCH_3)$), 121.5 (s, 1C; $CArC_p$), 128.4–129.0 (m; ArC), 129.4 (d; PArC), 130.2 (d; PArC), 132.3 (d, PArC), 138.1 (d, $^1J_{C,P}$ = 31.7 Hz, 2C; $PArC_{ipso}$), 153.3 (s, 1C; $CArC_{ipso}$), 222.6 (d, $^2J_{C,P}$ = 11.5 Hz, 4C; CO_{cis}), 345.2 (d, $^2J_{C,P}$ = 10.1 Hz, 1C; $C_{carbene}$); ^{31}P NMR (121.5 MHz): *cis* isomer: δ = 52.7; *trans* isomer: δ = 57.3; FT-IR (petroleum ether): *cis* isomer: $\tilde{\nu}$ = 2016 (m, C=O, A_1^2), 1928 (sh, C=O, A_1^1), 1915 (vs, C=O, B_1), 1893 cm^{-1}(m, br, C=O, B_2); *trans* isomer: $\tilde{\nu}$ = 2009 (w, C=O, A_{1g}), 1939 (m, C=O, B_{1g}), 1893 cm^{-1} (m, br, C=O, E_u); MS (FAB): m/z (%): 618 (4) [M^+], 590 (1) [$M^+ - CO$], 506 (100) [$M^+ - 4CO$], 386 (20) [$M^+ - 4CO - C(OCH_3)(C_6H_5)$]; MS (70 eV, EI): *m/z* (%): 506 (3) [$M^+ - 4CO$], 414 (2) [$M^+ - 3CO - C(OCH_3)(C_6H_5)$], 386 (9) [$M^+ - 4CO - C(OCH_3)(C_6H_5)$], 334 (33) [$M^+ - 4CO - CrC(OCH_3)(C_6H_5)$], 284 (4) [$CrC(OCH_3)(C_6H_5)^+$], 186 (57) [$HPPh_2^+$], 121 (100) [$(H_3CO)_3Si^+$]; HR-MS (EI): calcd for $C_{17}H_{23}O_3SiCrP$ [$M^+ - 4CO - C(OCH_3)(C_6H_5)$]: 386.0560; found 386.0570; calcd for $C_{12}H_8O_5Cr$-[$CrC(OCH_3)(C_6H_5)]^+$: 283.9777; found 283.9783.

***cis/trans*-Tetracarbonyl[(2-triethoxysilyl)ethyldiphenylphosphine][methoxy(phenyl)carbene]chromium(0) (5)**: A solution of carbene complex **1** (1.25 g, 4 mmol) and alkoxysilylphosphine **3** (1.51 g, 4 mmol) in diethyl ether (240 mL) was irradiated with a 150-W mercury lamp at −30 °C for 4 h under a flow of argon. The color of the solution changed from orange to dark red. The cold solution was filtered through celite, the volume was reduced to 20 mL and cooled to −60 °C. Precipitation of a red solid occurred which was filtered at −50 °C, washed with cold diethyl ether and dried under reduced pressure to afford pure *cis* isomer **5** as a red powder (1.66 g, 2.5 mmol, 61 %); m.p. 95 °C; R_f = 0.52 (petroleum ether/diethyl ether 2:1, −28 °C). In solution at room temperature partial isomerization occurred resulting in a 3:1 mixture of the *cis/trans* isomers. ^{1}H NMR (500 MHz, [D$_8$]toluene): *cis* isomer: δ = 0.77–0.89 (m, 2H; Si-CH_2), 1.10 (t, $^3J_{H,H}$ = 7 Hz, 9H; OCH_2CH_3), 2.67 (dt, $^2J_{H,P}$ = 13 Hz, $^3J_{H,H}$ = 4 Hz, 2H; P-CH_2), 3.40 (s, 3H; OCH_3), 3.70 (q, $^3J_{H,H}$ = 7 Hz, 6H; OCH_2CH_3), 6.65–6.68 (m; ArH), 6.87–7.14 (m; ArH), 7.56–7.61 (m; ArH); *trans* isomer: δ = 0.77–0.89 (m, 2H; Si-CH_2), 1.11 (t, $^3J_{H,H}$ = 7 Hz, 9H; OCH_2CH_3), 2.76 (dt, $^2J_{H,P}$ = 13 Hz, $^3J_{H,H}$ = 4 Hz, 2H; P-CH_2), 3.71 (q, $^3J_{H,H}$ = 7 Hz, 6H; OCH_2CH_3), 4.02 (s, 3H; OCH_3), 6.65–6.68 (m; ArH), 6.87–7.14 (m; ArH), 7.56–7.61 (m; ArH); ^{13}C NMR (125 MHz, [D$_8$]toluene): *cis* isomer: δ = 5.0 (d, $^2J_{C,P}$ = 2.4 Hz, 1C; Si-CH_2), 18.5 (s, 3C; OCH_2CH_3), 27.0 (d, $^1J_{C,P}$ = 18.7 Hz, 1C; P-CH_2), 58.6 (s, 3C; OCH_2CH_3), 63.8 (s, 1C; OCH_3), 128.4–130.4 (m; ArC), 132.7 (d, 2C; P-ArC_{ipso}), 153.4 (s, 1C; C-ArC_{ipso}), 221.5 (d, $^2J_{C,P}$ = 14.4 Hz, 2C; CO_{cis}), 226.4 (d, $^2J_{C,P}$ = 6.4 Hz, 1C; $CO_{trans\ to\ P}$), 232.4 (d, $^2J_{C,P}$ = 13.9 Hz, 1C; $CO_{trans\ to\ carbene}$), 348.8 (d, $^2J_{C,P}$ = 13.0 Hz, 1C; $C_{carbene}$); *trans* isomer: δ = 4.8 (d, 1C; Si-CH_2), 18.5 (s, 3C; OCH_2CH_3), 26.2 (d, $^2J_{C,P}$ = 18.7 Hz, 1C; P-CH_2), 58.6 (s, 3C; OCH_2CH_3), 65.8 (s, 1C; OCH_3), 128.4–130.4 (m; ArC), 132.4 (d, 2C; P-ArC_{ipso}), 153.4 (s, 1C; C-ArC_{ipso}), 222.6 (d, $^2J_{C,P}$ = 12.0 Hz, 4C; CO_{cis}), 345.0 (d, 1C; $C_{carbene}$); ^{31}P NMR (121.5 MHz): *cis* isomer: δ = 52.0, *trans* isomer: δ = 57.0; FT-IR (petroleum ether): *cis* isomer: $\tilde{\nu}$ = 2016 (m, C=O, A_1^2), 1928 (sh, C=O, A_1^1), 1915 (vs, C=O, B_1), 1894 cm^{-1} (m, C=O, B_2); *trans* isomer: $\tilde{\nu}$ = 2009 (sh, C=O, A_{1g}), 1940 cm^{-1} (m, C=O, B_2); MS (70 eV, EI): *m/z* (%): 568 (2) [$M^+ - CH_3 - C_6H_5$], 456 (10) [$M^+ - 3CO - C(OCH_3)(C_6H_5)$], 428 (60) [$M^+ - 4CO - C(OCH_3)(C_6H_5)$], 376 (42) [$M^+ - 4CO - CrC(OCH_3)(C_6H_5)$], 186 (100) [$HPPh_2^+$], 163 (92) [$(C_2H_5O)_3Si^+$]; $C_{32}H_{37}O_8CrPSi$ (660.7): calcd: C 58.17, H 5.64, Cr 7.87, P 4.69; found: C 58.01, H 5.55, Cr 7.79, P 4.49.

***cis*-Tetracarbonyl[(2-triethoxysilyl)ethyldiphenylphosphine][amino(phenyl)carbene]chromium(0) (13)**: Ammonia (3 mL) was condensed at −65 °C into a solution of **5** (0.23 g, 0.35 mmol) in diethyl ether (10 mL). Within 45 min the color of the solution changed from dark red to yellow. The solution was stirred for another hour to complete the reaction. After removal of the cooling bath the excess ammonia and the solvent were removed under reduced pressure. Crystallization from petroleum ether/

0947-6539/00/0616-3014 $ 17.50+.50/0 *Chem. Eur. J.* **2000**, *6*, No. 16

diethyl ether (3:1) gave orange crystals of **13** (0.13 g, 0.2 mmol, 57%); m.p. 97 °C; $R_f = 0.1$ (petroleum ether/diethyl ether 2:1, −28 °C). ^{1}H NMR (500 MHz, [D$_8$]toluene): $\delta = 0.68-0.79$ (m, 2H; Si-CH$_2$), 1.09 (t, $^2J_{H,H} =$ 7 Hz, 9H; OCH$_2$C*H*$_3$), 2.56 (dt, $^2J_{H,P} = 13$ Hz, $^3J_{H,H} = 4$ Hz, 2H; P-CH$_2$), 3.68 (q, $^3J_{H,H} = 7$ Hz, 9H; OC*H*$_2$CH$_3$), 6.50 (s, br., 2H; NH$_2$), 6.79–7.11 (m; ArH), 7.33–7.50 (m; ArH); ^{13}C NMR (125 MHz, [D$_8$]toluene): $\delta = 4.7$ (d, $^3J_{C,P} = 2.4$ Hz, 1C; Si-CH$_2$), 18.5 (s, 3C; OCH$_2$CH$_3$), 26.9 (d, $^2J_{C,P} = 18.2$ Hz, 1C; P-CH$_2$), 58.6 (s, 3C; O*C*H$_2$CH$_3$), 124.1 (s; C-ArC), 128.4–130.2 (m; ArC), 132.7 (d, $^2J_{C,P} = 9.6$ Hz; P-ArC), 137.2 (s; C-ArC), 137.4 (d, $^3J_{C,P} =$ 3 Hz; P-ArC), 153.3 (s, 1C; C-ArC$_{ipso}$), 222.0 (d, $^2J_{C,P} = 14.4$ Hz, 2C; CO$_{cis}$), 228.0 (d, $^2J_{C,P} = 5.3$ Hz, 1C; CO$_{trans\ to\ P}$), 229.9 (d, $^2J_{C,P} = 12.5$ Hz, 1C; CO$_{trans\ to\ carbene}$), 292.7 (d, $^2J_{C,P} = 11$ Hz, 1C; C$_{carbene}$); ^{31}P NMR (121.5 MHz): $\delta =$ 55.4; FT-IR (petroleum ether): $\tilde{\nu} = 2004$ (m, C=O, A$_1^2$), 1917 (s, C=O, A$_1^1$), 1898 (vs, C=O, B$_1$), 1882 cm^{-1} (s, C=O, B$_2$); MS (FAB): m/z (%): 645 (2) [M^+], 533 (100) [$M^+ - 4$CO], 456 (2) [$M^+ - 4$CO $-$ C$_6$H$_5$], 371 (19) [$M^+ -$ 4CO $-$ C(NH$_2$)(C$_6$H$_5$) $-$ C$_2$H$_5$ $-$ C$_2$H$_4$], 347 (15) [$M^+ -$ (CO)$_4$Cr(NH$_2$)-(C$_6$H$_5$) $-$ C$_2$H$_5$], 163 (5) [(C$_2$H$_5$O)$_3$Si$^+$]; C$_{31}$H$_{36}$O$_7$NCrPSi (645.68): calcd: C 57.66, H 5.62, N 2.17; found: C 57.72, H 5.63, N 2.15.

***cis*-Tetracarbonyl[(2-triethoxysilyl)ethyldiphenylphosphine][allylamino-(phenyl)carbene]chromium(0) (14)**: Allylamine (0.35 mL, 13 equiv) was added at −65 °C to a solution of **5** (0.23 g, 0.34 mmol) in diethyl ether (10 mL). After 0.5 h the reaction was completed (TLC control) and the color of the solution had changed from dark red to yellow. The cooling bath was removed and the residual allylamine and the solvent were removed under reduced pressure. Crystallization from petroleum ether/diethyl ether (3:1) gave yellow crystals of **13** (215 mg, 0.31 mmol, 91%); m.p. 72 °C; $R_f =$ 0.38 (petroleum ether/diethyl ether 2:1, −28 °C). ^{1}H NMR (500 MHz, [D$_8$]toluene): $\delta = 0.82$ (m, 2H; Si-CH$_2$), 1.10 (t, $^3J_{H,H} = 7$ Hz, 9H; OCH$_2$C*H*$_3$), 2.68 (dt, $^2J_{H,P} = 13$ Hz, $^3J_{H,H} = 4$ Hz, 2H; P-CH$_2$), 2.90 (br., 2H; N-CH$_2$), 3.70 (q, $^3J_{H,H} = 7$ Hz, 6H; OC*H*$_2$CH$_3$), 4.83 (m, 2H; =CH$_2$), 5.02–5.13 (m, 1H; CH$_2$-C*H*=), 6.65 (d; ArH), 6.88–7.11 (m; ArH), 7.53 (t; ArH), 8.08 (s, br., 1H; NH); ^{13}C NMR (125 MHz, [D$_8$]toluene): $\delta = 4.9$ (d, 1C; Si-CH$_2$), 18.6 (s, 3C; OCH$_2$CH$_3$), 27.4 (d, $^2J_{C,P} = 17.8$ Hz, 1C; P-CH$_2$), 52.4 (s, 1C; N-CH$_2$), 59.0 (s, 3C; O*C*H$_2$CH$_3$), 118.2 (s, 1C; =CH$_2$), 120.3 (s; ArC), 126.4 (s, 1C; HC=), 127.6–129.5 (m; ArC), 132.2 (s; ArC), 132.7 (d, $^2J_{C,P} = 9.6$ Hz; P-ArC), 137.4 (d, $^1J_{C,P} = 28.3$ Hz, 2C; P-ArC$_{ipso}$), 150.4 (s, 1C; C-ArC$_{ipso}$), 221.7 (d, $^2J_{C,P} = 13.9$ Hz, 2C; CO$_{cis}$), 228.1 (d, $^2J_{C,P} = 4.3$ Hz, 1C; CO$_{trans\ to\ P}$), 230.1 (d, $^2J_{C,P} = 13.4$ Hz, 1C; CO$_{trans\ to\ carbene}$), 287.1 (d, $^2J_{C,P} =$ 11.4 Hz, 1C; C$_{carbene}$); ^{31}P NMR (121.6 MHz): $\delta = 56.2$; FT-IR (petroleum ether): $\tilde{\nu} = 2003$ (m, C=O, A$_1^2$), 1918 (s, C=O, A$_1^1$), 1893 (vs, C=O, B$_1$), 1878 cm^{-1} (s, C=O, B$_2$); MS (FAB): m/z (%): 685 (1) [M^+], 573 (25) [$M^+ -$ 4CO], 532 (6) [$M^+ - 4$CO $-$ C$_3$H$_5$], 428 (100) [$M^+ - 4$CO $-$ C(NH(C$_3$H$_5$)(C$_6$H$_5$), 371 (22), 347 (17); C$_{34}$H$_{42}$O$_7$NCrPSi (687.77): calcd: C 59.38, H 6.16, N 2.04; found: C 59.4, H 6.00, N 2.38.

***cis*-Tetracarbonyl[(2-trimethoxysilyl)ethyldiphenylphosphine][allylamino-(phenyl)carbene]chromium(0) (15)**: Allylamine (0.029 g, 0.5 mmol, 1.1 equiv) was added at −55 °C to a solution of **4** (0.284 g, 0.46 mmol) in diethyl ether (6 mL). After 45 min the reaction was completed (IR, TLC control), while the color of the solution changed from dark red to orange. After the solution had been warmed to room temperature, evaporation of the solvent and chromatographic workup (eluent: petroleum ether/diethyl ether 2:1, −30 °C) yielded **15** as a viscous orange oil (0.28 g, 0.44 mmol, 95%); $R_f = 0.2$ (petroleum ether/diethyl ether 2:1). ^{1}H NMR (500 MHz, CDCl$_3$): $\delta = 0.48-0.62$ (m, 2H; Si-CH$_2$), 2.41 (dt, $^1J_{H,P} = 14$ Hz, $^3J_{H,H} =$ 4 Hz, 2H; P-CH$_2$), 3.25 (br., 2H; N-CH$_2$), 3.46 (s, 9H; OCH$_3$), 5.02–5.20 (m, 2H; =CH$_2$), 5.36–5.56 (m, 1H; C*H*=CH$_2$), 6.57 (d, 2H; ArH), 7.07–7.60 (m; ArH), 8.05 (s, br., 1H; NH); ^{13}C NMR (125 MHz, CDCl$_3$): $\delta =$ 2.67 (d, $^2J_{C,P} = 2.4$ Hz, 1C; Si-CH$_2$), 26.3 (d, $^1J_{C,P} = 17.7$ Hz, 1C; P-CH$_2$), 50.8 (s, 1C; N-CH$_2$), 52.5 (s, 3C; OCH$_3$), 119.6 (s, 1C; =CH$_2$), 120.6 (s, 1C; C-ArC), 127.0 (s, 1C; HC=), 128.7 (s, 1C; C-ArC), 129.2 (d, 2C; P-ArC), 130.1 (d, 2C; P-ArC), 132.6 (s, 1C; C-ArC), 137.6 (d, $^1J_{C,P} = 28.8$ Hz, 2C; P-ArC$_{ipso}$), 150.7 (s, 1C; C-ArC$_{ipso}$), 222.3 (d, $^2J_{C,P} = 13.9$ Hz, 2C; CO$_{cis}$), 229.0 (d, $^2J_{C,P} = 4.8$ Hz, 1C; CO$_{trans\ to\ P}$), 231.0 (d, $^2J_{C,P} = 13.4$ Hz, 1C; CO$_{trans\ to\ carbene}$), 288.1 (d, $^2J_{C,P} = 11.5$ Hz, 1C; C$_{carbene}$); ^{31}P NMR (121.5 MHz): $\delta =$ 55.6; FT-IR (petroleum ether): $\tilde{\nu} = 2004$ (m, C=O, A$_1^2$), 1918 (s, C=O, A$_1^1$), 1894 (vs, C=O, B$_1$), 1879 cm^{-1} (s, C=O, B$_2$); MS (FAB): m/z (%): 643 (4) [M^+], 587 (1) [$M^+ - 2$CO], 531 (52) [$M^+ - 4$CO], 490 (5) [$M^+ - 4$CO $-$ C$_3$H$_5$], 386 (100) [$M^+ - 4$CO $-$ C(NH(C$_3$H$_5$)(C$_6$H$_5$)], 371 (6) [$M^+ - 4$CO $-$ C(NH(C$_3$H$_5$)(C$_6$H$_5$) $-$ CH$_3$], 319 (27); MS (70 eV, EI): *m/z* (%): 386 (2) [$M^+ - 4$CO $-$ C(NH(C$_3$H$_5$)(C$_6$H$_5$)], 334 (42) [$M^+ - 4$CO $-$ CrC-(NH(C$_3$H$_5$)(C$_6$H$_5$)], 309 (6) [(CO)$_4$CrC(NH(C$_3$H$_5$)(C$_6$H$_5$)$^+$], 186 (91) [HPPh$_2^+$], 121 (100) [(H$_3$CO)$_3$Si$^+$]; HR-MS (EI): calcd. for C$_{17}$H$_{23}$O$_3$SiCrP [$M^+ - 4$CO $-$ C(NH(C$_3$H$_5$)(C$_6$H$_5$)]: 386.0560; found 386.0557; calcd for C$_{14}$H$_{11}$NO$_4$Cr [CrC(NH(C$_3$H$_5$)(C$_6$H$_5$)$^+$]: 309.0093; found 309.0094.

***cis*-Tetracarbonyl(2-triethoxysilyl)ethyldiphenylphosphine[isobutylamino-(phenyl)carbene]chromium(0) (16)**: Isobutylamine (0.12 mL, 1.1 equiv) was added at −68 °C to a solution of **5** (0.18 g, 0.27 mmol) in diethyl ether (7 mL). After 3 h the reaction was completed (TLC and IR control), while the color of the solution had changed from dark red to yellow. The cooling bath was removed and isobutylamine and the solvent were evaporated. Crystallization from petroleum ether/diethyl ether (3:1) gave yellow crystals of **16** (121 mg, 0.17 mmol, 64%); m.p. 56 °C; $R_f = 0.50$ (petroleum ether/diethyl ether. ^{1}H NMR (250 MHz, CDCl$_3$): $\delta = 0.55$ (m, 2H; Si-CH$_2$), 0.75 (d, $^3J_{H,H} = 7$ Hz, 6H; CH(C*H*$_3$)$_2$), 1.14 (t, $^3J_{H,H} = 7$ Hz, 9H; OCH$_2$C*H*$_3$), 1.53 (m, 1H; C*H*(CH$_3$)$_2$), 2.36–2.48 (m, 4H; P-CH$_2$, N-CH$_2$), 3.70 (q, $^3J_{H,H} = 7$ Hz, 6H; OC*H*$_2$CH$_3$), 6.58 (d, ArH), 7.10 (t, 2H; ArH), 7.25 (t, 4H; ArH), 7.33–7.55 (m, ArH), 8.03 (br, 1H; NH); ^{13}C NMR (62.5 MHz, CDCl$_3$): $\delta = 4.0$ (d, $^2J_{C,P} = 2.6$ Hz, 1C; Si-CH$_2$), 18.2 (s, 2C; CH(*C*H$_3$)$_2$), 19.6 (s, 3C; OCH$_2$*C*H$_3$), 26.3 (d, $^1J_{C,P} = 17.8$ Hz, 1C; P-CH$_2$), 28.5 (s, 1C; *C*H(CH$_3$)$_2$), 57.1 (s, 1C; N-CH$_2$), 58.4 (s, 3C; O*C*H$_2$CH$_3$), 120.2 (s, ArC), 126.1 (s, ArC), 127.8 (s, ArC), 128.4 (d, P-ArC), 129.2 (s, ArC), 132.4 (d, P-ArC), 136.7 (d, $^2J_{C,P} = 28.6$ Hz, 2C; P-ArC$_{ipso}$), 150.0 (s, 1C; C-ArC$_{ipso}$), 221.1 (d, $^2J_{C,P} = 14.3$ Hz, 2C; CO$_{cis}$), 227.9 (d, $^2J_{C,P} = 4.8$ Hz, 1C; CO$_{trans\ to\ P}$), 229.7 (d, $^2J_{C,P} = 14.0$ Hz, 1C; CO$_{trans\ to\ carbene}$), 284.3 (d, $^2J_{C,P} = 11.4$ Hz, 1C; C$_{carbene}$); ^{31}P NMR (121.6 MHz): $\delta = 56.8$; FT-IR (petroleum ether): $\delta =$ 2002 (m, C=O, A$_1^2$), 1917 (s, C=O, A$_1^1$), 1892 (vs, C=O, B$_1$), 1875 cm^{-1} (s, C=O, B$_2$); MS (FAB): *m/z* (%): 701 (1) [M^+], 589 (100) [$M^+ - 4$CO], 532 (7) [$M^+ - 4$CO $-$ C$_4$H$_9$], 428 (16) [$M^+ - 4$CO $-$ C(NH(C$_4$H$_9$)Ph)]; C$_{35}$H$_{44}$O$_7$NPCrSi (701.79): calcd: C 59.90, H 6.32, N 2.00; found: C 59.82, H 6.39, N 1.96.

***cis*-Tetracarbonyl(2-triethoxysilyl)ethyldiphenylphosphino[phenyl(pyrrolidino)carbene]chromium(0) (17)**: Pyrrolidine (0.55 mL, 13 equiv) was added at −65 °C to a solution of **5** (0.33 g, 0.5 mmol) in diethyl ether (10 mL). After 1 h the solution was allowed to warm to −30 °C and after another hour the reaction was completed (TLC and IR control). The color of the solution had changed from dark red to orange. The cooling bath was removed and the solvent and pyrrolidine were evaporated. Aminocarbene complex **17** was obtained as an orange oil which could not be further purified by chromatographic workup due to partial decomposition. $R_f =$ 0.43 (petroleum ether/diethyl ether 2:1); ^{1}H NMR (500 MHz, CDCl$_3$): $\delta =$ 0.49 (m, 2H; Si-CH$_2$), 1.13 (t, $^3J_{H,H} = 7$ Hz, 9H; OCH$_2$C*H*$_3$), 1.72 (pquin, $^3J_{H,H} = 7$ Hz, 2H; N-CH$_2$C*H*$_2$), 1.82 (pquin, $^3J_{H,H} = 7$ Hz, 2H; N-CH$_2$C*H*$_2$), 2.38 (dt, $^1J_{H,P} = 14$ Hz, $^3J_{H,H} = 4$ Hz, 2H; P-CH$_2$), 2.94 (t, $^3J_{H,H} = 7$ Hz, 2H; N-CH$_2$), 3.69 (q, $^3J_{H,H} = 7$ Hz, 6H; OC*H*$_2$CH$_3$), 3.82 (t, $^3J_{H,H} = 7$ Hz, N-CH$_2$), 6.33 (d, $^3J_{H,H} = 7.7$ Hz, 2H; 1,1′-Ar-H$_{carbene}$), 7.02 (t, $^3J_{H,H} = 7.5$ Hz, 1H; 3,3′-Ar-H$_{carbene}$), 7.16 (t, $^3J_{H,H} = 7.7$ Hz; 2,2′-Ar-H$_{carbene}$), 7.26–7.50 (m; ArH); ^{13}C NMR (125 MHz, CDCl$_3$): $\delta = 4.4$ (d, $^2J_{C,P} = 3.8$ Hz, 1C; Si-CH$_2$), 18.3 (s, 3C; OCH$_2$*C*H$_3$), 25.2 (s, 1C; N-CH$_2$*C*H$_2$), 25.5 (s, 1C; N-CH$_2$*C*H$_2$), 27.0 (d, $^1J_{C,P} = 17.7$ Hz, 1C; P-CH$_2$), 55.5 (s, 1C; N-CH$_2$), 58.8 (s, 3C; O*C*H$_2$CH$_3$), 59.2 (s, 1C; N-CH$_2$), 119.8 (s; ArC), 125.7 (s; ArC), 128.8 (s; ArC), 128.9 (d; P-ArC), 129.9 (s; ArC), 133.1 (d; P-ArC), 138.1 (d, $^1J_{C,P} =$ 26.4 Hz, 2C; P-ArC$_{ipso}$), 155.9 (s; C-ArC$_{ipso}$), 222.3 (d, $^2J_{C,P} = 14.4$ Hz, 2C; CO$_{cis}$), 228.8 (d, $^2J_{C,P} = 4.8$ Hz, 1C; CO$_{trans\ to\ P}$), 230.8 (d, $^2J_{C,P} = 12.0$ Hz, 1C; CO$_{trans\ to\ carbene}$), 277.8 (d, $^2J_{C,P} = 13.0$ Hz, 1C; C$_{carbene}$); ^{31}P NMR (202 MHz): $\delta = 52.4$; FT-IR (petroleum ether): $\delta = 2000$ (m, C=O, A$_1^2$), 1911 (s, C=O, A$_1^1$), 1886 (vs, C=O, B$_1$), 1876 cm^{-1} (s, C=O, B$_2$).

General procedure for the sol–gel process: Precursor complex **4**, **5**, or **15** (0.5 mmol) was dissolved in degassed ethanol (300 equiv), and degassed tetraalkoxysilane (15 equiv) was added. Hydrolysis and condensation reactions were started by adding an equimolar amount of water (with respect to the number of alkoxy groups) which contained 0.1 wt% of catalyst (NaF, NH$_4$OH). To guarantee homogeneity the solution was stirred until gelation occurred (15–90 min). The reaction mixture was allowed to age at room temperature for five days. Then the solvent was removed in vacuo. The resulting material was washed several times with diethyl ether and the solvent was evaporated at 10^{-4} Torr for 10 h.

11: Aqueous NaF catalyst (0.57 mL) was added to a suspension of **4** (309.3 mg, 0.5 mmol) and TMOS (1.142 g, 7.5 mmol) in ethanol (8.8 mL, 150 mmol). Gelation occurred within 17 min giving a dark red granulate-like material (860 mg). In the IR spectra in addition to the ν (CO) absorptions of the tetracarbonyl complex less intense ν(CO) absorptions of

a pentacarbonyl complex are observed. FT-IR (KBr): Tetracarbonyl carbene complex: $\tilde{\nu} = 2014$ (m, C=O, A_1^2), 1924 (sh, C=O, A_1^1), 1902 (vs, C=O, B_1), 1890 cm^{-1} (m, C=O, B_2); pentacarbonyl complex: $\tilde{\nu} = 2064$ (C=O, A), 1949 (C=O, E) cm^{-1}; ^{31}P CP-MAS NMR (161 MHz): $\delta = 52, -10$ $Ph_2P(CH_2)_2Si(OEt)_n(O_{1.5})_{3-n}$, 39 $-Ph_2P(O)(CH_2)_2Si(OEt)_n(O_{1.5})_{3-n}$; ^{13}C CP-MAS NMR (100 MHz): $\delta = 4.6$ (CH_2-Si), 16.6 (OCH_2CH_3), 24.0 (P-CH_2), 50.6 (Si-CH_2), 59.3 (Si-OCH_2CH_3), 65.7 (C-OCH_3), 129.8 (ArC), 208.8 ($C_{carbonyl}$).

12: FT-IR (KBr): Tetracarbonyl carbene complex: $\tilde{\nu} = 2015$ (m, C=O, A_1^2), 1926 (sh, C=O, A_1^1), 1909 (vs, C=O, B_1), 1890 cm^{-1} (m, C=O, B_2); pentacarbonyl complex: $\tilde{\nu} = 2065$ (C=O, A), 1948 (C=O, E) cm^{-1}.

18: FT-IR (KBr): Tetracarbonyl carbene complex: $\tilde{\nu} = 2001$ (m, C=O, A_1^2), 1908 (sh, C=O, A_1^1), 1881 cm^{-1} (m, C=O, B_1, B_2); pentacarbonyl complex: $\tilde{\nu} = 2064$ (C=O, A), 1948 (C=O, E) cm^{-1}.

General procedure for the aminolysis of tetracarbonyl[methoxy(phenyl)-carbene]chromium(0) immobilized on silica: The starting material (200 mg) was suspended in diethyl ether (5–7 mL) and amine (allylamine, isobutylamine, pyrrolidine) (0.5–1 mL) was added at $-65\,^{\circ}C$. The suspension was shaken from time to time and warmed slowly to $-25\,^{\circ}C$, while the color changed from red to yellow-brown. After three days the solvent was decanted and the gel was washed several times with diethyl ether and dried in vacuo to give a yellow-brown granulate which was characterized by FT-IR (KBr): (In addition to the absorption pattern of the tetracarbonyl complex, unchanged absorption bands of a pentacarbonylcomplex are observed.)

20: Tetracarbonyl carbene complex: $\tilde{\nu} = 2000$ (m, C=O, A_1^2), 1905 (s, C=O, A_1^1), 1880 cm^{-1} (m, C=O, B_1, B_2); pentacarbonyl complex: $\tilde{\nu} = 2063$ (C=O, A), 1944 (C=O, E) cm^{-1}.

21: Tetracarbonyl carbene complex: $\tilde{\nu} = 2000$ (m, C=O, A_1^2), 1905 (s, C=O, A_1^1), 1879 (vs, C=O, B_1), 1869 cm^{-1} (sh, C=O, B_2); pentacarbonyl complex: $\tilde{\nu}(CO) = 2063$ (C=O, A), 1944 (C=O, E) cm^{-1}.

22: Tetracarbonyl carbene complex: $\tilde{\nu} = 1997$ (m, C=O, A_1^2), 1899 (s, C=O, A_1^1), 1877 (vs, C=O, B_1), 1870 cm^{-1} (sh, C=O, B_2); pentacarbonyl complex: $\tilde{\nu} = 2063$ (C=O, A), 1946 (C=O, E) cm^{-1}.

24: Tetracarbonyl carbene complex: $\tilde{\nu} = 2000$ (m, C=O, A_1^2), 1908 (s, C=O, A_1^1), 1882 cm^{-1} (m, C=O, B_1, B_2); pentacarbonyl complex: $\tilde{\nu} = 2063$ (C=O, A), 1943 (C=O, E) cm^{-1}.

25: Tetracarbonyl carbene complex: $\tilde{\nu} = 2000$ (m, C=O, A_1^2), 1907 (s, C=O, A_1^1), 1881 (s, C=O, B_1), 1870 cm^{-1} (sh, C=O, B_2); pentacarbonyl complex: $\tilde{\nu} = 2064$ (C=O, A), 1942 (C=O, E) cm^{-1}.

26: Tetracarbonyl carbene complex: $\tilde{\nu} = 1996$ (m, C=O, A_1^2), 1899 (s, C=O, A_1^1), 1879 (s, C=O, B_1, B_2); pentacarbonyl complex: $\tilde{\nu} = 2063$ (C=O, A), 1945 (C=O, E) cm^{-1}.

Reaction of ammonia with Tetracarbonyl[methoxy(phenyl)carbene]chromium(0) immobilized on silica: At $-70\,^{\circ}C$ 3 mL of ammonia was condensed into a suspension of the starting material (200 mg) in diethyl ether (3 mL). After 4 h the residual ammonia and the solvent were removed in vacuo affording a yellow-brownish granulate.
FT-IR(KBr): (In addition to the absorption pattern of the tetracarbonyl complex, unchanged absorption bands of a pentacarbonylcomplex are observed.)

19: Tetracarbonyl carbene complex: $\tilde{\nu} = 2000$ (m, C=O, A_1^2), 1905 (s, C=O, A_1^1), 1885 (s, C=O, B_1), 1877 cm^{-1} (s C=O, B_2); pentacarbonyl complex: $\tilde{\nu} = 2062$ (C=O, A), 1948 (C=O, E) cm^{-1}.

23: Tetracarbonyl carbene complex: $\tilde{\nu} = 2001$ (m, C=O, A_1^2), 1905 (s, C=O, A_1^1), 1883 cm^{-1} (s C=O, B_1, B_2); pentacarbonyl complex: $\tilde{\nu} = 2064$ (C=O, A), 1944 (C=O, E) cm^{-1}.

Acknowledgement

Financial support provided by the Fonds der Chemischen Industrie and the Ministry of Science and Research NRW is gratefully acknowledged.

[1] W.-C. Haase, K. H. Dötz, *Tetrahedron Lett.* **1999**, *40*, 2919.
[2] a) E. O. Fischer, A. Maasböl, *Angew. Chem.* **1964**, *76*, 645; *Angew. Chem. Int. Ed. Engl.* **1964**, *3*, 580; b) E. O Fischer, *Adv. Organomet. Chem.* **1976**, *14*, 1; c) K. H. Dötz, H. Fischer, P. Hofmann, F. R. Kreissl, U. Schubert, K. Weiss, *Transition Metal Carbene Complexes*, VCH, Weinheim, **1983**.
[3] a) K. H. Dötz, *Angew. Chem.* **1984**, *96*, 573; *Angew. Chem. Int. Ed. Engl.* **1984**, *23*, 587; b) W. D. Wulff in *Comprehensive Organic Synthesis*, *Vol. 5*, Pergamon, Oxford, **1991**, 1065; c) L. S. Hegedus, *Tetrahedron* **1997**, *53*, 4105; d) K. H. Dötz, J. Pfeiffer in *Transition Metals for Organic Synthesis*, *Vol. 1* (Eds.: M. Beller, C. Bolm), Wiley-VCH, Weinheim, **1998**, p. 335; e) F. Zaragoza Dörwald, *Metal Carbenes in Organic Synthesis*, Wiley-VCH, Weinheim, **1999**.
[4] a) R. Hoffmann, *Angew. Chem.* **1982**, *94*, 725; *Angew. Chem. Int. Ed. Engl.* **1982**, *21*, 711; b) F. G. A. Stone, *Angew. Chem.* **1984**, *96*, 85; *Angew. Chem. Int. Ed. Engl.* **1984**, *23*, 89.
[5] a) C. C. Kreiter, *Angew. Chem*. **1968**, *80*, 402; *Angew. Chem. Int. Ed. Engl.* **1968**, *7*, 390; b) C. P. Casey, W. R. Brusold, D. M. Scheck, *Inorg. Chem.* **1977**, *16*, 3059.
[6] a) W. D. Wulff, S. R. Gilbertson, *J. Am. Chem. Soc.* **1985**, *107*, 503; b) W. D. Wulff, Y. C: Xu, *J. Org. Chem.* **1987**, *52*, 3263; c) T. S. Powers, Y. Shi, K. J. Wilson, W. D. Wulff, A. Rheingold, *J. Org. Chem.* **1994**, *59*, 6882.
[7] a) E. Nakamura, K. Tanaki, T. Fujimura, S. Aoki, P. G. Williard, *J. Am. Chem. Soc.* **1993**, *115*, 9015; b) J. Barluenga, J. M. Monserrat, J. Flórez, S. García-Granda, E. Martin, *Chem. Eur. J.* **1995**, *1*, 236; c) W. D. Wulff in *Comprehensive Organometallic Chemistry II*, *Vol. 12* (Eds.: E. W. Abel, F. G. A. Stone, G. Wilkinson), Pergamon Press, New York, **1995**, p. 469.
[8] a) W. D. Wulff, W. E. Banta, R. W. Kaesler, P. J. Lankford, R. A. Miller, C. K. Murray, D. C. Uang, *J. Am. Chem. Soc.* **1990**, *112*, 3642; b) B. A. Anderson, W. D. Wulff, T. S. Powers, S. Tributt, A. L. Rheingold, *J. Am Chem. Soc.* **1992**, *114*, 10784.
[9] Recent review: K. H. Dötz, P. Tomuschat, *Chem. Soc. Rev.* **1999**, *28*, 187.
[10] J. Pfeiffer, M. Nieger, K. H. Dötz, *Eur. J. Org. Chem.* **1998**, 1011.
[11] Recent reviews: a) A. Fürstner, *Top. Catal.* **1997**, *4*, 285; b) R. H. Grubbs, S. J. Miller, G. C. Fu, *Acc. Chem. Res.* **1995**, *28*, 446; c) M. Schuster, S. Blechert, *Angew. Chem.* **1997**, *109*, 2124; *Angew. Chem. Int. Ed. Engl.* **1997**, *36*, 2036.
[12] a) K. G. Allum, R. D. Handcock, I. V. Howell, S. McKenzie, R. C. Pitkethly, P. J. Robinson, *J. Organomet. Chem.* **1975**, *87*, 203; b) D. C. Bailey, S. H. Langer, *Chem. Rev.* **1981**, *81*, 109; c) E. Lindner, T. Schneller, F. Auer, H. A. Mayer, *Angew. Chem.* **1999**, *111*, 2288; *Angew. Chem. Int. Ed.* **1999**, *38*, 2154.
[13] S. Maiorana, P. Seneci, T. Rossi, C. Baldoli, M. Ciraco, E. de Magistris, E. Licandro, A. Papagni, S. Provera, *Tetrahedron Lett.* **1999**, *40*, 3635.
[14] a) H. D. Gesser, P. C. Goswami, *Chem. Rev.* **1989**, *89*, 765; b) L. L. Hench, J. K. West, *Chem. Rev.* **1990**, *90*, 33; c) C. J. Brinker, G. W. Scherer, *Sol-Gel Science: The Physics and Chemistry of Sol-Gel Processing*; Academic Press, New York, **1990**.
[15] a) U. Schubert, *New J. Chem.* **1994**, *18*, 1049; b) D. A. Ward, E. I. Ko, *Ind. Eng. Chem. Res.* **1995**, *34*, 421; c) M. G. L. Petrucci, A. K. Kakkar, *Adv. Mater.* **1996**, *8*, 251.
[16] U. Schubert, N. Hüsing, A. Lorenz, *Chem. Mater.* **1995**, *7*, 2010.
[17] a) E. J. A. Pope, J. D. Mackenzie, *J. Non-Cryst. Solids* **1986**, *87*, 185; b) C. J. Brinker, *J. Non-Cryst. Solids* **1988**, *100*, 31; c) U. Schubert, K. Rose, *J. Non-Cryst. Solids* **1988**, *105*, 165; d) F. Ehrburger-Dolle, J. Dallamano, E. Elaloui, G. M. Pajonk, *J. Non-Cryst. Solids* **1995**, *186*, 9; e) S. Hæreid, M. Dahle, S. Lima, M.-A. Einarsrud, *J. Non-Cryst. Solids* **1995**, *186*, 96; f) M.-A. Einarsrud, M. B. Kirkedelen, E. Nilsen, K. Mortensen, J. Samseth, *J. Non-Cryst. Solids* **1998**, *231*, 10.
[18] a) R. Uriarte, T. J. Mazanec, K. D. Tau, D. W. Meek, *Inorg. Chem.* **1980**, *19*, 79; b) D. K. Liu, M. S. Wrighton, D. R. McKay, G. E. Maciel, *Inorg. Chem.* **1984**, *23*, 212.
[19] E. O. Fischer, H. Fischer, *Chem. Ber.* **1974**, *107*, 657.
[20] U. Schubert, E. O. Fischer, *Chem. Ber.* **1973**, *106*, 3882.
[21] R. Aelion, A. Loebel, F. Eirich, *J. Am. Chem. Soc.* **1950**, *72*, 5702.
[22] D. C. Bailey, S. H. Langer, *Chem. Rev.* **1981**, *81*, 143.
[23] N. Hüsing, U. Schubert, *Chem. Mater.* **1998**, *10*, 3024.
[24] a) R. A. Komoroski, A. J. Magistro, P. P. Nicholas, *Inorg.Chem.* **1986**, *25*, 3917; b) A. Lorenz, G. Kickelbick, U. Schubert, *Chem. Mater*. **1997**, *9*, 2551.
[25] a) M. Mägi, E. Lippmaa, A. Samoson, G. Engelhardt, A.-R. Grimmer, *J. Phys. Chem.* **1984**, *88*, 1518; b) E. Lippmaa, M. Mägi, A. Samoson, M. Tarmak, E. Engelhardt, *J. Am. Chem. Soc.* **1981**, *103*, 4992.

  0947-6539/00/0616-3016 $ 17.50+.50/0

[26] a) B. S. Shukla, G. P. Johari, *J. Non-Cryst. Solids* **1988**, *101*, 263; b) B. Himmel, H. Bürger, Th. Gerber, Olbertz, *J. Non-Cryst. Solids* **1995**, *185*, 56.
[27] G. M. Pajonk, A. V. Rao, B. M. Sawant, N. N. Parvathy, *J. Non-Cryst. Solids* **1997**, *207*, 40.
[28] R. K. Iler, *The Chemistry of Silica*, Wiley, New York, **1979**, p. 175.
[29] S. Brunauer, L. S. Deming, W. S. Deming, E. Teller, *J. Am. Ceram. Soc.* **1940**, *62*, 1723.
[30] a) P. A. Webb, C. Orr, *Analytical Methods in Fine Particle Technology*, Micromeritics Instrument Corporation, Norcross GA USA, 53; b) C. J. Brinker, G. W. Scherer, *Sol-Gel Science: The Physics and Chemistry of Sol-Gel Processing*, Academic, New York, **1990**.
[31] E. P. Barrett, L. G. Joyner, P. P. Halenda, *J. Am. Chem. Soc.* **1951**, *73*, 373.
[32] H. Werner, E. O. Fischer, B. Heckl, C. G. Kreiter, *J. Organomet. Chem.* **1971**, *28*, 367.
[33] A. Brenner, D. A. Hucul, S. J. Hardwick, *Inorg. Chem.* **1979**, *18*, 1478.
[34] J. A. Connor, E. O. Fischer, *J. Chem. Soc. (A)* **1969**, 578.
[35] a) review: U. Schubert, *Coord. Chem. Rev.* **1984**, *55*, 261; b) O. S. Mills, A. D. Redhouse, *J. Chem. Soc. A* **1969**, 1274.
[36] D. F. Harvey, D. M. Sigano, *Chem. Rev.* **1996**, *96*, 271.
[37] a) J. P. A. Harrity, W. J. Kerr, *Tetrahedron* **1993**, *49*, 5565; b) T. J. Katz, G. X. Q. Yang, *Tetrahedron Lett.* **1991**, *32*, 5895.
[38] For a similar linking strategy see [13] and S. E. Gibson, N. J. Hales, M. A. Peplow, *Tetrahedron Lett.* **1999**, *40*, 1417.
[39] E. O. Fischer, A. Maasböl, *Chem. Ber.* **1967**, *100*, 2445.

Received: November 9, 1999 [F2129]